

Thermodynamics of compact-star matter within an Ising approach

P. Chomaz^a, C. Ducoin^{ab}, F. Gulminelli^{b*}, K. Hasnaoui^a and P. Napolitani^{ab}

^aGanil(DSM-CEA/IN2P3-CNRS), Blvd. H. Becquerel, BP 55027, F-14076 Caen cédex5, France

^bLPC(IN2P3-CNRS/Ensicaen et Université), F-14076 Caen cédex, France

In the formation and evolution of compact stars, nuclear matter explores high thermal excursions and is the site of intense neutrino emission. Neutrino transport as well as structural properties of this matter depend on the presence of inhomogeneous phases (named “pasta” phases), which are the result of Coulomb frustration of the Liquid-Gas phase transition. We take into account charge fluctuations by employing a frustrated lattice-gas model to which we impose a neutrality constraint by the addition of an homogeneous background of charge, representing delocalised electrons. Within this schematic model we highlight a generic feature of the phase-transition phenomenology: the temperature interval where pasta phases are formed is enhanced by Coulomb-frustration effects. This result is at variance with the behaviour of frustrated ferromagnetic systems as well as hot nuclei and mean-field approaches. Moreover, the region of phase coexistence is not found to end upon a critical point, indicating that no critical opalescence can occur in compact-star matter.

1. Introduction: stars and atomic nuclei

Nuclear matter present in compact and hot astrophysical objects generated in a gravitational collapse suffers from high thermal excursions. In the accessible range of temperature and densities, nuclear matter presents phase transitions characterized by density fluctuations. Because of the presence of the long range Coulomb interaction, those charge fluctuations give rise to so called “frustration effects” [1]. Under these conditions, the system organises in inhomogeneous phases, named “pasta phases” due to their unusual topologies [2]. The evolution of these structures with density is expected to be connected to the properties of the inner neutron-star crust. The survival of pasta-phases at finite temperature has been inferred from recent molecular-dynamics simulations [4]. As these complex structures are related to coherent neutrino scattering [3], their evolution with density and temperature or, more generally, the underlying equation of state, becomes a key quest for exploring several interconnected astrophysical phenomena, like the dynamics of supernova explosion and the thermodynamics of proto-neutron-stars cooling.

A tempting connection can be searched with the physics of atomic nuclei, which are experimentally accessible. Comparable conditions of temperature and density can be

*member of the Institut Universitaire de France

probed in rather violent processes like nuclear multifragmentation. However, compact-star matter differs from normal nuclear matter due to the presence of electrons. They constitute an incompressible degenerated gas, which establishes a condition of global charge neutrality at large scale.

To understand the phenomenology of phase transitions in compact stars, we consider an Ising model. Indeed widely used mean-field approximations [5, 6, 7] are known to fail to describe critical phenomena in 3D. The Ising model is specifically suited for the analysis of charge fluctuations by exact calculations, since phase transitions are universal phenomena. Moreover, it was largely employed in the study of ferromagnetic systems subjected to frustration [10] as well as for nuclear matter [9] where, in the form of the lattice-gas model, magnetic spins are replaced by site occupations.

2. Ising analogue to compact-star matter

We construct a cubic periodic lattice composed of V sites, each characterised by a position \mathbf{i} and an occupation number $n_{\mathbf{i}} = 1$ or 0 , to indicate the presence or the absence of positive charge, respectively. This distribution of positive charge simulates the distribution of nuclear-matter charge (neutron and protons without distinction are considered as nucleons with an effective charge Z/A). The strongly incompressible gas of electrons is represented by a uniform distribution of negative charge [11] imposing a strict condition of neutrality. In any site we find therefore an effective charge $q_{\mathbf{i}} = n_{\mathbf{i}} - \bar{n}$, where $\bar{n} = \sum_{\mathbf{j}}^V n_{\mathbf{j}}/V$ is the charge per site of the background of negative charge.

The schematic Hamiltonian $\mathcal{H}_{n+C} = \mathcal{H}_n + \mathcal{H}_C$ with

$$\mathcal{H}_n = \frac{\epsilon}{2} \sum_{\mathbf{i}, \mathbf{j}}' n_{\mathbf{i}} n_{\mathbf{j}}, \quad \mathcal{H}_C = \frac{\lambda \epsilon}{2} \sum_{\mathbf{i} \neq \mathbf{j}} \frac{q_{\mathbf{i}} q_{\mathbf{j}}}{r_{\mathbf{ij}}} \quad (1)$$

is introduced to study the interplay of nuclear-like (\mathcal{H}_n) and Coulomb-like forces (\mathcal{H}_C). $\sum_{\mathbf{i}, \mathbf{j}}'$ is a sum extended over closest neighbors, and $r_{\mathbf{ij}}$ is the distance between sites \mathbf{i} and \mathbf{j} . The short-range and long-range interactions are characterized by the coupling constants ϵ and $\lambda \epsilon = \alpha \hbar c \rho_0^{1/3} x^2$ respectively, where ρ_0 is the nuclear saturation density, and x is the proton fraction. The ratio of the two coupling constants λ measures the strength of frustration. In the sequel, x is fixed to $1/3$, a value expected for proto-neutron stars. \mathcal{H}_C can be rewritten in terms of occupation products times the geometric constants $C_{\mathbf{ij}}$ as

$$\mathcal{H}_C = \frac{\lambda \epsilon}{2} \sum_{\mathbf{i}, \mathbf{j}} n_{\mathbf{i}} n_{\mathbf{j}} C_{\mathbf{ij}}. \quad (2)$$

Translational invariance, which is ensured by imposing the distance $\mathbf{r}_{\mathbf{ij}}$ to be the shortest between \mathbf{i} and \mathbf{j} in the periodic space, imposes $\sum_{\mathbf{i}}^V C_{\mathbf{ij}} = 0$. Hence, $C_{\mathbf{ij}}$ can be calculated by adopting periodic boundary conditions in the form

$$C_{\mathbf{ij}} = D_{\mathbf{ij}} - \mathcal{D}, \quad \text{with} \quad \mathcal{D} = \frac{1}{V} \sum_{\mathbf{i}'}^V D_{\mathbf{0i}'}, \quad (3)$$

where $D_{\mathbf{ij}} = 0$ if $\mathbf{i} = \mathbf{j}$, and $D_{\mathbf{ij}} = |\mathbf{r}_{\mathbf{ij}}|^{-1}$ otherwise; \mathcal{D} is calculated with respect to any position $\mathbf{0}$.

\mathcal{H}_C preserves all the characteristic symmetries of the Ising model and the Coulomb energy is therefore invariant for lattice-occupation reversal. We should also point out that, despite some tempting similarities, the correspondent of eq.(1) in spin variable $s_i = n_i - 1/2$ and $\rho = \mathcal{M}/V + 1/2$ with the magnetization $\mathcal{M} = \sum_i^V s_i$ is not identical to the Hamiltonian of the frustrated Ising ferromagnet [10], defined by

$$\mathcal{H}_{\text{Fe}} = \frac{\epsilon}{2} \sum_{i,j}^V s_i s_j + \frac{q\epsilon}{2} \sum_{i,j}^V s_i s_j D_{ij}. \quad (4)$$

Indeed, \mathcal{H}_{Fe} and \mathcal{H}_{n+C} are related by

$$\mathcal{H}_{\text{Fe}} = \mathcal{H}_{n+C} + \frac{\lambda\epsilon}{2} \mathcal{D} \mathcal{M}^2 + 3\epsilon \mathcal{M} - \frac{3\epsilon}{4} V, \quad (5)$$

This connection includes a term in \mathcal{M}^2 , scaling with V^2 . Such term deeply modifies the thermodynamics in a finite system, and imposes $\mathcal{M} = 0$ at the thermodynamic limit for \mathcal{H}_{Fe} . The strict constraint $\mathcal{M} = 0$ on the order parameter \mathcal{M} leads to a substantial modification of the thermodynamics of the system[13]. The phase diagram of the frustrated ferromagnet [10], where , as in nuclei, the Coulomb interaction reduces the phase-coexistence region (i.e. decreases the limiting temperature), cannot be directly exported to our system \mathcal{H}_{n+C} .

3. Simulation in the multi-grandcanonical ensemble

For the numerical simulation of the \mathcal{H}_{n+C} system, in order to take into account the long-range Coulomb interactions in a rapidly converging form, the finite lattice is repeated in

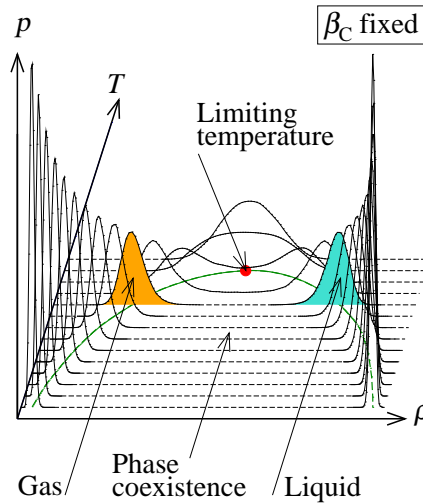


Figure 1. Example of a Metropolis calculation ($\mu = \mu_c$). Density distribution for a fixed value of β_C and a series of temperatures, each one associated to one spectrum. The ensemble of explored temperatures and densities defines the phase diagram. The ridge of the distribution defines three branches joining at the limiting temperature. The phase-coexistence region is delimited by the gas (low density) and liquid (high density) branches.

all three directions of space a large number R of times. Each site \mathbf{i} has R replicas of itself, each one displaced from \mathbf{i} of a vector $\mathbf{m}L$, where \mathbf{m} has integer components and $L = \sqrt[3]{V}$.

To treat a frustrated system, described by the interplay of several interactions, the multi-(grand) canonical ensemble[9] is specifically suited. It consists in associating a Lagrange multiplier to each component of the Hamiltonian that we want to treat as a separate observable. In particular, it makes possible to construct one single phase diagram for both neutral and charged matter by associating one Lagrange multiplier, β_n , to the nuclear energy (related to \mathcal{H}_n) and another, β_C , to the Coulomb energy E_C (related to \mathcal{H}_C). The multi-canonical partition sum reads:

$$Z_{\beta_n, \beta_C, V}(\rho V, V) = \int W_V(E_n, E_C, \rho V, V) e^{-\beta_n E_n - \beta_C E_C} dE_n dE_C, \quad (6)$$

where $W_V(E_n, E_C, \rho V, V)$ is the density of states. For any finite value of β_C , we treat the system as equilibrated at the temperature $T = 1/\beta_n$ and described by an equivalent effective charge $q_{\text{eff}}^2 = \lambda \beta_C / \beta_n$. When $\beta_C = 0$, the Coulomb energy E_C does no more influence the partition sum and the system behaves as uncharged, reducing to the standard Ising model. The generalised grand potential is defined as

$$Z_{\beta_n, \beta_C, \alpha}^G(V) = \int Z_{\beta_n, \beta_C}(\rho V, V) e^{-\alpha \rho V} d\rho, \quad (7)$$

where the fugacity is linked to the chemical potential by $\alpha = -\beta_n \mu$. When $\beta_C = \beta_n$ the ensemble coincides with the conventional grand-canonical form.

We sampled the density distribution from eq.(7) for a chemical potential value $\mu = \mu_c = 3\epsilon$, by employing a standard Metropolis technique [14]. An example is presented in Fig. 1 where, for a fixed value of β_C , several density distributions are calculated for different temperatures $T = 1/\beta_n$. All bimodal distributions present a peak for the gas phase (low-density) and one for the liquid (high-density) phase. Their height is equal because of the choice of $\mu = \mu_c$. All distributions are composed together to draw a phase diagram: the ridge of the overall distribution of density and temperature delimits with its gas branch and liquid branch the phase coexistence. The two branches join at the limiting temperature.

4. Results

For two cases, either $\beta_n = 0$ (corresponding to the standard Ising model), or $\beta_n = \beta_C$, and for a series of different lattice sizes L , we collected a series of calculations of the phase diagram. The results are schematized in Fig. 2. The phase-coexistence region in the system $\beta_n = 0$ shrinks for progressively larger lattice sizes according to the characteristic finite-size scaling behaviour of the Ising system. In particular, since the asymptotic value of the limiting temperature $T_{\text{lim}} = \lim_{L \rightarrow \infty} \dot{T}_{\text{lim}}(L)$ corresponds to a critical point, finite-size scaling requires that $\dot{T}_{\text{lim}}(L)$ evolves as $\dot{T}_{\text{lim}}(L) - T_{\text{lim}} \propto L^{-1/\nu}$ [15]. This is confirmed by the calculated values of the critical exponent ν and the critical point T_{lim} , which correspond to the Ising values.

At variance with the Ising behaviour, the phase diagram of the system $\beta_n = \beta_C$ does however not vary with the lattice size. This first sign of incompatibility of the frustrated system with the Ising model, is also a first indication of quenching of the critical behaviour.

ν rules in fact the divergence of the correlation length at the critical point, which evolves as $\xi \propto t^{-\nu}$ with $t = T/T_{\text{lim}} - 1$. If a critical point existed, it would correspond to a very large value for ν , which would then be hardly compatible with a diverging correlation length.

The major result we infer from comparing the two systems and the corresponding asymptotic limiting temperature, is that the coexistence region expands under the action of a Coulomb field.

The connection between the increase of the limiting point and charge fluctuations can be searched in the evolution of the event distribution with temperature and Coulomb-field strength. Fig. 3A illustrates the evolution of the limiting temperature with the strength of the Coulomb field and the phase coexistence is indicated for the uncharged system $\beta_C = 0$ and the frustrated system $\beta_C = \beta_n$, in correspondence with the phase diagrams shown in Fig. 2. We analyzed the event distribution along the path 1-2-3-4, determined by four different thermodynamic situations.

In Fig. 3B the distributions are shown, as a function of the two Hamiltonian components, $(1/2V) \sum_{i,j}^V n_i n_j$ and $(\lambda/2V) \sum_{i \neq j}^V q_i q_j / r_{ij}$. Point (1) belongs to the region of phase coexistence sampled for the uncharged system $\beta_C = 0$ and presents a bimodal pattern with respect to the abscissa, which corresponds to the nuclear-energy density E_n/V , so that pure liquid or gas partitions are preferred to mixed events. Point (2) corresponds to the limiting temperature of the uncharged system $\beta_C = 0$, where mixed partitions are favoured. To pass from point (2) to point (3) the temperature is left unchanged while β_C is increased from 0 till it equals β_n . Once introduced the Coulomb field, $(\lambda/2V) \sum_{i \neq j}^V q_i q_j / r_{ij}$ represents the Coulomb-energy density E_C/V , which should be minimized in the frustrated system. In order to satisfy this constraint, the positive-charge distribution searches

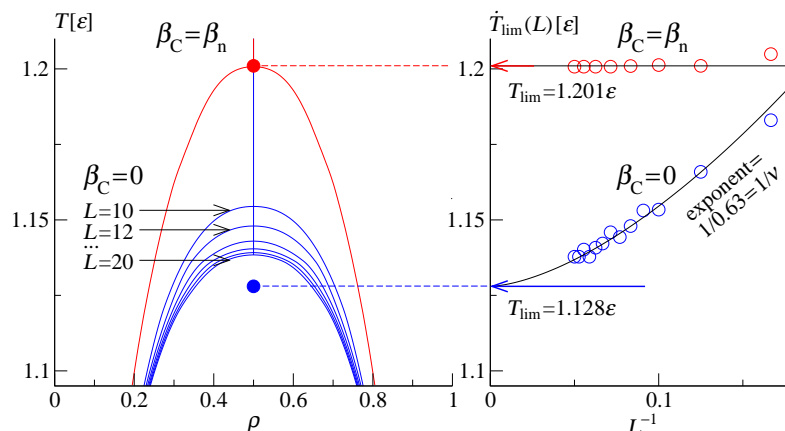


Figure 2. **Left panel.** Calculations of phase diagrams for the systems $\beta_n = 0$ (Ising-like) and $\beta_n = \beta_C$ (frustrated). Calculations for a series of different lattice sizes L are associated to different limiting temperatures for the system $\beta_n = 0$; they overlap for the system $\beta_n = \beta_C$. **Right panel.** For the system $\beta_n = 0$ the test of the finite-size scaling law $T_{\text{lim}}(L) - T_{\text{lim}} \propto L^{-1/\nu}$ gives Ising values for the critical exponent ν and the critical temperature T_{lim} . No scaling is observed for the system $\beta_n = \beta_C$: this is a first indication of the quench of criticality in presence of a Coulomb field.

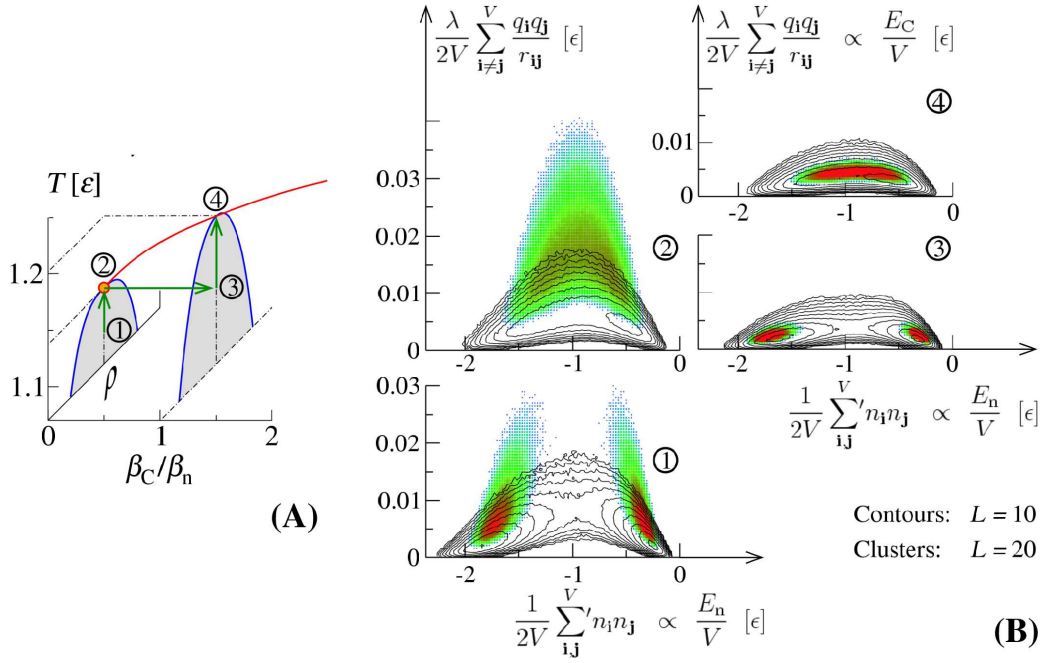


Figure 3. **(A)** Increase of the limiting point and expansion of the phase-coexistence region with increasing frustration (i.e. for higher β_C/β_n ratios). Four points determine different thermodynamical situations: points (1) and (3) belong to the coexistence region, points (2) and (4) are at the limiting temperature; while points (1) and (2) refer to the system $\beta_C = 0$ (Ising-like), points (3) and (4) refer to the system $\beta_C = \beta_n$ (frustrated). The calculation refers to $L = 10$; **(B)** In correspondence with the points marked in panel (A), the probability distribution is evaluated for the two Hamiltonian components, $(1/2V) \sum_{i,j}^V n_i n_j$, which corresponds to the nuclear-energy density E_n/V , and $(\lambda/2V) \sum_{i \neq j}^V q_i q_j / r_{ij}$, representing the Coulomb-energy density E_C/V in the case of the frustrated system. Contour plots refer to $L = 10$; logarithmic cluster plots refer to $L = 20$. Points (1) and (3) manifest bimodal patterns. The critical scaling effect exhibited at point (2) quenches at point (4).

uniform patterns, which are better compensated by the uniform background of negative charges. As a result, the system moves to the phase-coexistence region to search pure partitions, and bimodality appears. In the frustrated system, the temperature should be further increased with respect to the limiting temperature of the system $\beta_C = 0$, point (3), in order to find the limiting temperature, as indicated at point (4).

Fig. 3B presents the event distributions sampled for two different lattice sizes, in order to test scaling effects which could indicate the presence of critical points. At a critical point the correlation length ξ diverges and determines the exponential decay of the correlation function $\sigma(\mathbf{r}_{\mathbf{i},\mathbf{j}}) = \langle n_{\mathbf{i}}n_{\mathbf{j}} \rangle - \langle n_{\mathbf{i}} \rangle \langle n_{\mathbf{j}} \rangle$ according to the expression $\sigma(r) \propto e^{-r/\xi} \cdot r^{-(D-2+\eta)}$, where D is the space dimension and η is a critical exponent. On the basis of the properties of the $C_{\mathbf{i},\mathbf{j}}$ matrix, $\sigma(r)$ is related to the mean Coulomb-energy density by

$$\left\langle \frac{\lambda\epsilon}{2V} \sum_{\mathbf{i} \neq \mathbf{j}}^V \frac{q_{\mathbf{i}}q_{\mathbf{j}}}{r_{\mathbf{i},\mathbf{j}}} \right\rangle = \left\langle \frac{E_C}{V} \right\rangle = \frac{\lambda\epsilon}{2} \left(\sigma(0)\mathcal{D} + \sum_{\mathbf{j} \neq \mathbf{0}}^V \frac{\sigma(\mathbf{r}_{\mathbf{0},\mathbf{j}})}{r_{\mathbf{0},\mathbf{j}}} \right). \quad (8)$$

It is therefore typical of a critical point to exhibit a divergence of the quantity $\langle \sum_{\mathbf{i} \neq \mathbf{j}}^V q_{\mathbf{i}}q_{\mathbf{j}}/r_{\mathbf{i},\mathbf{j}} \rangle$ for progressively larger lattice sizes. This indicates that, at point (2), the limiting point is compatible with a critical point, as we already expected from the finite-size scaling law tested in Fig. 2 for the critical exponent ν . On the contrary, no scaling is observed at the point (4). Indeed, as indicated by Eq.(8), when the Coulomb field is introduced in the system, the diverging quantity would be the Coulomb-energy density E_C/V . To avoid such a singularity, the correlation length keeps a finite value at the limiting temperature and the critical character of the limiting temperature is lost [16]. A more formal discussion on the suppression of criticality on the basis of finite-size-scaling analysis is presented in ref. [17].

5. Conclusions

By employing a specific model for studying the thermodynamical features of a frustrated system, we could define general properties of a neutral system in presence of charge fluctuations, in analogy to compact-star matter. The study of the phase diagram and the phase-transition phenomenology indicated that the introduction of a Coulomb field has the effect of increasing the limiting temperature without preserving any critical character.

This result is the opposite as found for many other physical systems subject to Coulomb frustration in the absence of global charge neutrality, from hot atomic nuclei to frustrated ferromagnets [8, 18, 10, 19, 9]. This discrepancy with the phase-transition phenomenology characteristic of atomic nuclei, indicates that a connection between compact-star matter and nuclei is not trivial. Conversely a widening of the density range connected to the pasta phases was found [11] within the RMF model, when the Coulomb field is included under the constraint of global charge neutrality over the Wigner-Seitz cells. Such a finding is directly compatible with the thermodynamic phenomenology we are drawing.

It was also discussed [20, 21] that neutrino propagation can be highly concerned by the presence of pasta phases and characterizes the process of neutron-star formation and cooling. With respect to homogeneous phases, the inhomogeneous phases (like pasta phases) present in the coexistence region are characterized by a larger opalescence to neutrino propagation. In the presence of a critical point the opalescence would diverge as

a direct consequence of the divergence of the correlation length, and neutrinos would be trapped. On the contrary, we conclude that the medium stays “grey” at any temperature. This result seems also connected to the observation of small opacity for the transport of neutrinos discussed in ref. [22].

REFERENCES

1. J.W. Negele and D. Vautherin, Nucl. Phys. A **207**, 298 (1973).
2. D.G. Ravenhall, C.J. Pethick, and J.R. Wilson, Phys. Rev. Lett. **50**, 2066 (1983); M. Lassaut *et al.*, Astron. Astrophys. **183** L3 (1987); C.J. Pethick and D.G. Ravenhall, Annu. Rev. Nucl. Part. Sci. **45**, 429 (1995); G. Watanabe *et al.*, Nucl.Phys. A **676**, 455 (2000); N.K. Glendenning, Phys. Rep. **342**, 393 (2001); J.M. Lattimer and M. Prakash, Phys. Rep. **333**, 121 (2000).
3. C. Horowitz *et al.*, Phys. Rev. C **70**, 065806 (2004).
4. G. Watanabe *et al.*, Phys. Rev. Lett. **94**, 031101 (2005); C.J. Horowitz *et al.*, Phys. Rev. C **69**, 045804 (2004).
5. J.M. Lattimer *et al.*, Nucl. Phys. A **432**, 646 (1985).
6. F. Douchin, P. Haensel and J. Meyer, Nucl. Phys. A **665**, 419 (2000).
7. C. Ducoin *et al.*, to be published.
8. P. Bonche, S. Levit and D. Vautherin, Nucl. Phys. A **436**, 265 (1985).
9. F. Gulminelli *et al.*, Phys. Rev. Lett. **91**, 202701 (2003).
10. M. Grousson, G. Tarjus and P. Viot, Phys. Rev. E **62**, 7781 (2000); Phys. Rev. E **64**, 036109 (2001).
11. T. Maruyama *et al.*, Phys. Rev. C **72**, 015802 (2005).
12. J. Barré, D. Mukamel and S. Ruffo, Phys. Rev. Lett. **87** 030601 (2001).
13. F. Gulminelli *et al.*, Phys. Rev. E **68**, 026120 (2003).
14. Ph. Chomaz, F. Gulminelli, in “*Dynamics and thermodynamics of systems with long range interactions*”, Lecture Notes in Physics vol.**602**, Springer (2002).
15. K. Binder, “*Monte Carlo Methods in Statistical Mechanics*”, 2nd ed. Berlin: Springer-Verlag (1986).
16. Ph. Chomaz *et al.*, arXiv:astro-ph/0507633 (2005).
17. P. Napolitani *et al.*, in preparation.
18. S.J. Lee, A.Z. Mekjian, Phys. Rev. C **63**, 044605 (2001).
19. Al.H. Raduta, Ad.R. Raduta, Nucl. Phys. A **703**, 876 (2002).
20. J. Margueron, J. Navarro and P. Blottiau, Phys. Rev. C **70**, 28801 (2004).
21. G. Watanabe, H. Sonoda, AIP Conf. Proc. **791**, 101 (2005).
22. C.J. Horowitz, and J. Piekarewicz, Phys. Rev. C **72**, 035801 (2005).